JOURNAL OF SOLID STATE CHEMISTRY 112, 243–250 (1994)

Orientational Disorder and Heterogeneous Reaction Behavior of NO_2^- and NO_3^- Anions Inside a Sodalite Matrix

J.-C. Buhl[1] and J. Löns

Institut für Mineralogie, Universität Münster, Corrensstrasse 24, W-48149 Münster, Federal Republic of Germany

Received August 17, 1993; in revised form November 17, 1993; accepted November 18, 1993

The crystallization of nitrite/nitrate enclathrated sodalite solid solutions has been investigated under hydrothermal conditions in the system Na_2O–SiO_2–Al_2O_3–$NaNO_2$–H_2O. The oxidation potential within the silver-lined autoclaves at elevated temperatures ($T \geq 773$ K) and pressures ($p \geq 0.15$ GPa) gives rise to the formation of a temperature dependent nitrite/nitrate ratio within the crystals. Structural investigations on nitrite/nitrate sodalite have been carried out using IR spectroscopy, MAS NMR as well as single crystal structure refinement. Considering both of the imbibed anions have a "rigid body" their real positions within the sodalite cages could be found. Besides synthesis and the structural characterization the heterogeneous reaction behavior of nitrite/nitrate sodalite in a CO_2 atmosphere has also been investigated. At elevated temperatures (1073 K) a total anion exchange could be established, yielding to the formation of carbonate sodalite.

INTRODUCTION

The aluminosilicate framework of sodalite group minerals is formed by an alternating connection of corner-sharing SiO_4 and AlO_4 tetrahedra. Their linkage gives rise to the space filling array of $[4^6 6^8]$ polyhedral cages. These β cages can accommodate several guest anions and cations. Sodalites with a wide variety of guest anions have been synthesized in recent times, but most of them imbibed only one anion type (1–5). Future applications of sodalites as nanocomposites and special host matrices for new quantum dot materials (6–10) are requiring the enclathration of mixed anions within one sodalite matrix, but the question on the homogeneity of the distribution of different cage fillings over the whole crystal is still open. Besides the possibility of formation of a homogeneous solid solution the evaluation of nitrite and nitrate enriched domains over the whole crystal must also be taken into account. In order to reach a better understanding of this problem we continue our studies on the incorporation of different oxoanions into the sodalite matrix by studying the mechanism of synthesis and the structural properties of nitrite/nitrate sodalite solid solutions.

Nitrite/nitrate enclathrated sodalite has been recently prepared via intracage oxidation of initial grown pure nitrite sodalite (11–13) or by hydrothermal synthesis (13). Polycrystalline material and single crystals have been characterized by X-ray powder diffraction, IR-spectroscopy as well as simultaneous thermoanalysis in argon or in air (13). To continue these studies, this paper reports on structural investigations of nitrite/nitrate sodalite by IR spectroscopy, MAS NMR and single crystal X-ray structure refinement. The aim of this work is to answer the question about the structural arrangement of the nitrite and nitrate anions inside the β cages as well as to clarify the problem of the distribution of these different cage fillings over the whole crystal.

Besides synthesis and the structural characterization the heterogeneous reaction behavior of nitrite/nitrate sodalite in a CO_2 atmosphere has also been investigated.

EXPERIMENTAL

Synthesis and Characterization

Hydrothermal syntheses have been carried out in the system Na_2O–SiO_2–Al_2O_3–$NaNO_2$–H_2O. The starting amount of sodium nitrite as well as the temperature and pressure were varied to determine the conditions of nitrite/nitrate formation during crystal growth. Syntheses were performed in 18 ml steel autoclaves, using silver liners (100 mm length; 8 mm diameter) as sample containers. These liners were filled with 50 mg Kaolin (Fluka 60609), sintered at 1673 K. Different amounts of $NaNO_2$ (Riedel-de Haen 31443) were added together with 1 ml of an 8 *M* NaOH. The autoclaves were heated in a special vertical cylinder furnace. A pressure up to 0.2 GPa, estimated from the Kennedy diagram, was controlled by the degree of filling. After a reaction period of 48 hr single crystalline products could be observed exclusively. The

[1] To whom correspondence should be addressed.

0022-4596/94 $6.00

TABLE 1
Conditions of the Hydrothermal Syntheses and the Reaction Products Obtained

No.	Quantity of $NaNO_2$ (mg)	Temperature (K)	Pressure (GPa)	Products[a]
1	69	573	0.1	OH/NO_2–SOD
2	276	573	0.1	NO_2–SOD
3	69	648	0.1	OH/NO_2–SOD
4	276	648	0.1	NO_2–SOD
5	69	773	0.15	$OH/NO_2/NO_3$–SOD
6	276	773	0.15	NO_2/NO_3–SOD
7	69	873	0.15	$OH/NO_2/NO_3$–SOD
8	276	873	0.15	NO_2/NO_3–SOD
9	69	973	0.20	$OH/NO_2/NO_3$–SOD
10	276	973	0.20	NO_2/NO_3–SOD

[a] NO_2–SOD: Nitrite sodalite $Na_8[AlSiO_4]_6(NO_2)_2$. OH/NO_2–SOD: Basic nitrite sodalite $Na_8[AlSiO_4]_6(NO_2)(OH \cdot H_2O)$. $OH/NO_2/NO_3$–SOD: Basic nitrite/nitrate sodalite $Na_8[AlSiO_4]_6(NO_2)_{1-x}(NO_3)_x$ $(OH \cdot H_2O)$, $0.2 \leq x \leq 0.9$. NO_2/NO_3–SOD: Nitrite/nitrate sodalite solid solution $Na_8[AlSiO_4]_6(NO_2)_{2-x}(NO_3)_x$; $0.4 \leq x \leq 1.8$: Refined unit cell constants: $x = 0$: $a_0 = 8.931(2)$ Å, $x = 0.4$: $a_0 = 8.952(1)$ Å, $x = 1.0$: $a_0 = 8.962(2)$ Å, $x = 1.8$: $a_0 = 8.989(1)$ Å.

various parameters of syntheses are summarized in Table 1.

The products were characterized by X-ray powder diffraction, using a Guinier–Jagodzinski camera (Cu-$K_{\alpha 1}$ radiation, internal Si standard). The cell parameters of the synthesized phases were calculated by least squares refinement.

The cage filling species nitrite and nitrate, water molecules, hydroxyl groups as well as impurities of carbonate from the mother liquor were distinguished by means of IR spectroscopy, using a Perkin–Elmer spectrometer 683 (KBr pellets). The degree of filling of the sodalite cages with the guest species has been checked by thermogravimetry in connection with IR spectroscopy and X-ray diffraction. A detailed thermoanalytical study of nitrite–nitrate sodalite solid solutions was given elsewhere (13).

In order to characterize the heterogeneous reaction behavior of nitrite/nitrate sodalite 100 mg of fine grained sodalite powder have been heated in a CO_2 stream of 5 l/h for different times at 973 K as well as 1073 K. The Mettler thermoanalyzer TA 146 has been used for these heating experiments.

The ^{29}Si MAS NMR spectra of a selected sample of nitrite/nitrate sodalite was recorded on a Bruker CXP-300 FT NMR spectrometer, equiped with an MAS NMR probehead at 59.5 MHz using a single pulse sequence with 2–3 μsec pulse duration and 3–7 sec pulse delay. The spinning rate was 4 kHz. The chemical shift was related to tetramethylsilane standard.

The ^{23}Na MAS NMR spectrum was recorded at 105.8 MHz and 1-μsec pulse duration with 4 sec repetition on a Bruker MSL 400 MAS NMR spectrometer. The chemical shift was related to crystalline NaCl.

Structure Refinement

The crystal structure of nitrite/nitrate sodalite has been refined, using a dodecahedral shaped crystal of average dimensions of 0.15 mm. This crystal was taken from the batch No. 8, Table 1, having an average chemical composition of $Na_8[AlSiO_4]_6(NO_2)(NO_3)$ with the cubic unit cell parameter $a_0 = 8.962(2)$ Å. Precession photographs show reflections, consistent with space group symmetry $P\bar{4}3n$. The Enraf-Nonius four-circle diffractometer CAD 4 has been revealed for the data collection (Mo$K\alpha$1 radiation, graphite monocromator). 17814 independent reflections were collected up to a 2θ maximum of 120° ($\theta/2\theta$-scan mode). Lorentz polarization and spherical absorption correction have been applied to the measured data. The unit cell parameter has been determined from least squares refinement, using 25 reflections in the 4–60° range of 2θ. 1157 reflections with intensities $I > 3\ \sigma(I)$ have been selected. Sixty-six free structural parameters were refined, including an overall scale factor as well as an isotropic extinction parameter. The experimental details are summarized in Table 2.

RESULTS

Synthesis

The results of the hydrothermal syntheses are given in Table 1. No oxidation reaction has been observed at low

TABLE 2
Crystallographic Data and Experimental Conditions for the Structure Refinement of Nitrite/Nitrate Sodalite $Na_8[AlSiO_4]_6(NO_2)(NO_3)$

Crystal size and shape	0.15 mm, rhombendodecahedral
Data collection	
Temperature	295 K
Number of reflections	17,814
8409 reflections in the 2θ range and range of reciprocal space	$4° \leq 2\theta \leq 60°$ $-17 \leq h \leq 17$ $-17 \leq k \leq 17$ $-7 \leq l \leq 7$
9405 reflections in the 2θ range and range of reciprocal space	$60° \leq 2\theta \leq 150°$ $0 \leq h \leq 25$ $0 \leq k \leq 25$ $-10 \leq l \leq 10$
Cell parameter calculated from 25 reflections in the 2θ range of 4–60°	$a_0 = 8.958(1)$ Å, $Z = 1$
Number of reflections after Data reduction	1157 [$I > 3\,\sigma(I)$]
Space group	$P\bar{4}3n$
R value (unweighted)	2.8%
R value (weighted)	1.6%
Number of refined parameters	66

temperatures in the 573–648 K intervall for the samples Nos 1–4; here only nitrite sodalite occurs. Nitrite/nitrate-imbibed sodalite could be synthesized at high temperatures and pressures, as can be seen from the experiments Nos. 5–10 in Table 1. The oxidation potential within the silver-lined autoclaves at elevated temperatures ($T \geq 773$ K) and pressures ($p \geq 1.5$ GPa) has found to be responsible for the formation of a temperature-dependent nitrite–nitrate ratio within the crystals. The silver metal of the same liners plays the important role to produce an oxygen partial pressure, required for the observed nitrate formation. The following reaction scheme can be therefore proposed (14):

$$2Ag^+ + 2OH^- \rightarrow 2AgOH \rightarrow Ag_2O + H_2O$$

$$Ag_2O \rightarrow 2Ag + \tfrac{1}{2}O_2$$

$$NO_2^- + \tfrac{1}{2}O_2 \rightarrow NO_3^-$$

Nitrite/nitrate sodalites could be synthesized in the composition range of $Na_8[AlSiO_4]_6(NO_2)_{2-x}(NO_3)_x$; 0, $4 \leq x \leq 1{,}8$. The cell parameter of the nitrite/nitrate sodalites from Table 1 are also included in this table. Low nitrite concentrations in the starting materials of the hydrothermal syntheses always yield complex sodalite solid solutions, containing hydroxide–hydrate ($NaOH \cdot H_2O$) beside nitrite and/or nitrate. All products contain more or less amounts of carbonate impurities, imbibed from the NaOH solution during synthesis. The unit cell parameter of those samples is always somewhat higher than that for the pure ones.

Unlike as in the initial nitrate-containing system (5) a sodalite–cancrinite cocrystallization does not exist by using $NaNO_2$ in the starting substances. The synthesis, described here, yields single crystals of good quality as compared with very low crystal perfection of nitrite/nitrate sodalites from high-temperature oxidation experiments of primary grown nitrite sodalites (11–13), so that a single crystal structure refinement of nitrite–nitrate sodalite could be carried out here.

IR Spectroscopy and MAS NMR

A product of the composition $Na_8[AlSiO_4]_6(NO_2)(NO_3)$ has been selected for all the structural investigations. The IR spectrum of this phase is shown in Fig. 1a, whereas Figs. 1b and 1c illustrate the spectra of basic nitrite/nitrate sodalite (No. 5, Table 1) and basic nitrite sodalite (No. 1, Table 1). In the mid-infrared region the symmetric and asymmetric T–O–T vibrations of the sodalite framework appear. The positions of the symmetric T–O–T stretching modes differ somewhat as a function of the framework expansion of the sodalites, as already shown by Henderson and Taylor for several other salt-filled sodalites (15). Thus the IR spectroscopic results clearly indicate the more expanded character of the framework with higher nitrate content within the sodalite cages (wavenumbers of the symmetric T–O–T stretching modes: 733 709, and 664 cm^{-1} for pure nitrite sodalite and 730, 705, and 660 cm^{-1} for nitrite/nitrate sodalite).

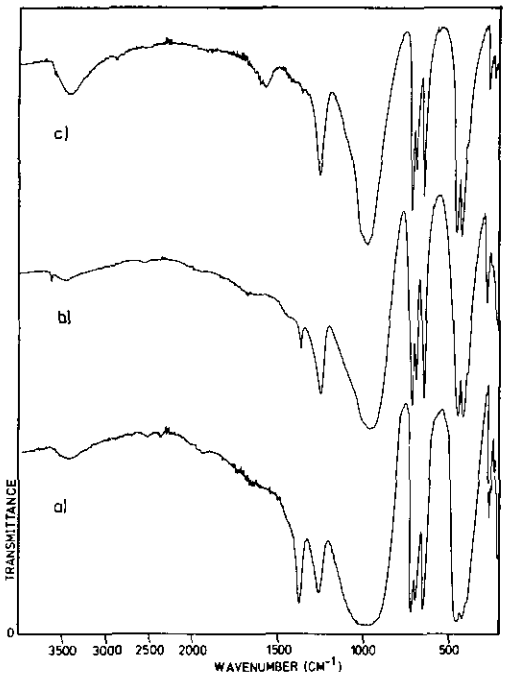

FIG. 1. IR spectra of the reaction products: (a) nitrite/nitrate sodalite (No. 8, Table 1), (b) basic nitrite/nitrate sodalite (No. 5, Table 1), (c) basic nitrite sodalite hydrate (No. 1, Table 1).

The enclathrated guests can be detected according to their intensive absorption bands at 1260 cm^{-1} (NO_2^-), 1385 cm^{-1} (NO_3^-) and 1450 cm^{-1} (CO_3^{2-} impurities from the NaOH solution of the synthesis). The imbibition of $NaOH \cdot H_2O$ at low nitrite contents in the starting materials (Figs. 1b and 1c) is shown by a 3640 cm^{-1} stretching mode from the terminal OH groups of the [H–O ··· H ··· O–H]$^-$ anion (16), whereas the expected brought stretching vibration of the central strong hydrogen bonded O ··· H overlaps with the asymmetric stretching mode of the imbibed traces of carbonate (impurities of the NaOH solution from synthesis) as well as with the framework vibrations at wavenumbers ≤ 1200 cm^{-1}, as recently described by Engelhardt *et al.* and Wiebcke *et al.* for basic sodalite (16, 17). The imbibed water molecules also can be detected from the IR spectra (absorption band at 3100 cm^{-1}–3600 cm^{-1} and 1650 cm^{-1} in Fig. 1c).

Figure 2a shows the ^{29}Si MAS NMR spectrum of the nitrite/nitrate sodalite. As can be seen from this figure, ^{29}Si MAS NMR confirms the alternating Si, Al ordering of the framework according to a single line at $\delta = -86.20$ ppm for Si(4Al) units and an Si/Al ratio of 1,0. The ^{29}Si MAS NMR spectra of pure nitrite sodalite as well as pure nitrate sodalite are already known from literature (3, 5). Each of these spectra is also exhibiting a single sharp peak with a highly symmetrical line shape and a chemical shift of $\delta = -85.5$ ppm for nitrite sodalite as well as $\delta = -86.7$ ppm for nitrate sodalite. From the shape of the ^{29}Si MAS NMR spectra of nitrite/nitrate sodalite in Fig. 2a one can assume, that domains of nitrite sodalite or nitrate sodalite do not exist in the structure and that on the contrary the different cage fillings exhibit the character of a regular solid solution over the whole crystal.

The ^{23}Na MAS NMR spectrum of nitrite/nitrate sodalite is given in Fig. 2b. It shows a broad line according to second order quadrupolar interactions. The deviations from the typical quadrupole pattern with two maxima are a result from field gradients inside the sodalite cages, influenced by the dynamics of the enclathrated guest species. As can be further seen from Fig. 2b the resonance signal exhibits an unsymmetrical line shape in the high-field direction. This indicates deviations in the chemical environment of the sodium cations according to the different nature of the enclathrated guests nitrite and nitrate.

Structure Refinement of Nitrite/Nitrate Sodalite

For all structural calculations the Programm SHELX (18) has been used. The atomic scattering factors for neutral atoms were taken from (19), whereas the initial positional parameters were chosen from the single crystal refinement of sodium chloride sodalite (20). After the location of the framework atoms Si, Al, and O(1) in a first

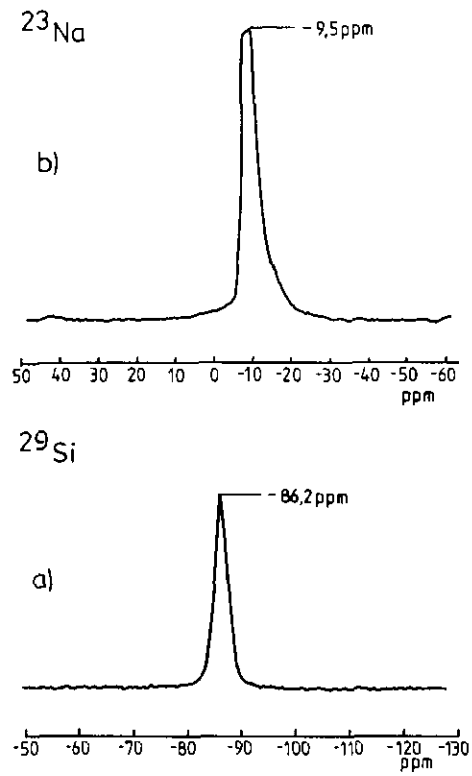

FIG. 2. MAS NMR spectra of nitrite/nitrate sodalite: (a) ^{29}Si MAS NMR spectrum, (b) ^{23}Na MAS NMR spectrum.

refinement (space group $P\bar{4}3n$), the positions of the nonframework atoms were taken from the results of difference Fourier calculations according to peaks on sites 2*a* (0, 0, 0) and 24*i* (*x*, *y*, *z*). The nitrogen atoms were placed in the center position 2*a*, whereas the oxygens of the cage filling nitrite and nitrate anions have been positioned on the 24-fold general (24*i*) site. Due to remaining electron density from difference Fourier maps after the refinement of this structure model the 12-fold (*x*, 0, 0) average position for one out of the three oxygen atoms of the nitrate has been included in the model. Large isotropic displacement parameters of the nonframework atoms (N and O) and residual electron density in difference Fourier maps on sites (0, 0, 0) and (*x*, *x*, *x*) clearly indicated an off-center position for the *N* atoms. Despite the goodness of fit between the structural parameters on the basis of this model, the calculated interatomic distances and angles of the imbibed guest anions showed major deviations compared with the geometry of these groups in solid $NaNO_2$ (N–O = 1.240 Å, O–N–O = 115° (21) and solid $NaNO_3$ (N–O = 1.254 Å, O–N–O = 120° (22, 23). These contrasts are caused by the 12-fold disorder of the enclathrated anions within the sodalite cages, making a detailed study of the position of one single group highly impossible. Figure 3 illustrates the positional disorder of both types of anions schematically. To overcome these difficulties, constraints for the bonding distances and angles of the nitrate and nitrate group were applied, considering the NO_2^- and the NO_3^- as a rigid body with regular geometry, found in the solid sodium salts of these anions. Therefore the real position of the guests could be revealed. During the final procedure of this rigid body refinement the constraints could be replaced by restraints for the bond lengths within an optional σ range. The atomic parameters and the isotropic temperature factors of the final refinement together with all e.s.d.'s are included in Table 3. Selected interatomic distances and bond angles are summarized in Table 4. As known from sodalites with other guest anions, the framework of nitrite/nitrate sodalite consists of completely ordered AlO_4 and SiO_4 tetrahedra, with a Si–O–Al bonding angle of 142.6(1)° and a Si/Al ratio of 1.0. in a good agreement with the ^{29}Si MAS NMR data, discussed above.

Three independent but close sodium sites could be refined, all placed on the 8*e* position of SG $P\bar{4}3n$, i.e., located on the body diagonals, close to the six membered rings of AlO_4 and SiO_4 tetrahedra of the framework. These split positions, found in a refinement with free parameters for the cation positions and occupancies are giving a hint on differences in the strength of the Na–N and Na–O(1) interactions within the sodalite cages, either filled with the nitrate or nitrite. Whereas the Na3 position belongs to the cations located in the nitrite filled cages, the arrangement of the planar nitrate anion is responsible for

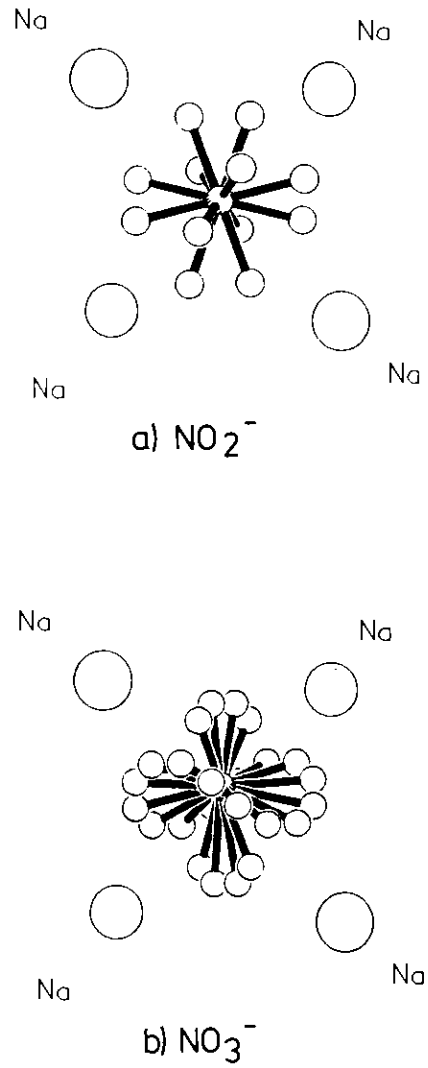

FIG. 3. Model of the positional disorder of the nitrite and nitrate anions within the tetrahedral arrangement of the sodium cations in the sodalite cages (N atom located at the center position 0, 0, 0; not all the O atoms of the oxoanions are apparent.)

the Na1 and Na2 sites according to an occupancy ratio of ≈3 : 1 within every NO_3^- containing cage. The split model of the sodium cations provides the best fit to the experimental data, compared with a refinement on the basis of only one average sodium position.

One out of the twelve possible positions of the nitrite and the nitrate anions within the tetrahedral arrangement of the sodium cations in the sodalite cages are shown in Figs. 4a and 4b.

The *N* atoms of both anions are located in an off-center position within the β-cages. The same 12-fold disordered positions, already known from structural investigations of pure nitrite sodalites (24, 25) could also be stated for the nitrite within the mixed crystal. On the contrary the

TABLE 3
Fractional Coordinates and Equivalent Displacement Parameters with e.s.d.'s of Nitrite/Nitrate Sodalite

Atom	Site	Occupancy	x	y	z	U_{eq}[a]
			Aluminosilicate framework			
Si	6*d*	1,0	0,250	0,000	0,500	0,00647(7)
Al	6*c*	1,0	0,250	0,500	0,000	0,00666(8)
O1	24*i*	1,0	0,14101(5)	0,44574(5)	0,1509(1)	0,0123(1)
Na1	8*e*	0,3650(9)	0,18229(7)	0,18229(7)	0,1829(7)	0,0259(7)
Na2	8*e*	0,1485(6)	0,2026(7)	0,2026(7)	0,2026(7)	0,0258(7)
Na2	8*e*	0,4729(5)	0,1909(5)	0,1909(5)	0,1909(9)	0,0194(6)
			Nitrate			
N1	24*i*	0,0481(6)	0,4926(10)	0,5174(11)	0,5090(12)	0,131(2)[b]
O21	24*i*	0,0481(6)	0,3543(7)	0,4965(12)	0,4757(9)	0,022(1)[b]
O22	24*i*	0,0481(6)	0,5571(9)	0,4287(10)	0,6021(9)	0,025(1)[b]
O23	24*i*	0,0481(6)	0,5667(11)	0,6243(11)	0,4482(12)	0,093(1)[b]
			Nitrite			
N2	24*i*	0,0359(7)	0,4943(10)	0,5037(10)	0,4956(13)	0,033(1)[b]
O31	24*i*	0,0359(7)	0,3681(10)	0,4581(10)	0,4612(12)	0,025(1)[b]
O32	24*i*	0,0359(7)	0,5268(11)	0,6288(10)	0,4458(12)	0,032(2)[b]

[a] $(U_{eq} = (1/24^2)\, i\, j\, B_{ij} a_i * a_j * a_i a_j$.
[b] Isotropic refinement.

nitrate group is positioned with one of its three edges parallel to a face of the tetrahedron of the sodium cations (Fig. 4b).

From these positions of both types of anions a highly dynamic character of the imbibed groups can be suggested to prevent an apparent polarization among the guests inside a sodalite cage as already discussed by Kempa *et al.* for pure nitrite sodalite (24).

TABLE 4
Selected Interatomic Distances (Å) and Angles (°) of Nitrite/Nitrate Sodalite

	Aluminosilicate framework		
Si–O1	1.6190(0)	Al–O1	1.737(0)
O1–Si–O1 (2×)	113.5(0)	O1–Al–O1 (2×)	111.6(0)
O1–Si–O1 (4×)	107.5(0)	O1–Al–O1 (4×)	108.4(0)
Si–O1–Al	141.4(0)		
Na1–O1	2.405(4)	Na2–O1	2.294(3)
Na3–O1	2.353(3)		
	Na coordination		
Na1–O31	2.427(14)		
Na1–O32	2.248(14)		
Na2–O21	2.494(14)		
Na3–O21	2.330(12)	Na3–O23	2.514(13)
Na3–O31	2.509(13)	Na3–O32	2.370(12)
NO_3^-–anion			
N1–O21	1.288(15)	O21–N1–O22	119.5(9)
N1–O22	1.288(16)	O21–N1–O23	120.4(10)
N1–O23	1.287(17)	O22–N1–O23	120.1(9)
NO_2^-–anion			
N2–O31	1.241(13)	O31–N–O32	115.0(1)
N2–O32	1.241(13)		

From these positions of both types of anions a highly dynamic character of the imbibed groups can be suggested

Heterogeneous Reaction Behavior of Nitrite/Nitrate Sodalite in a CO_2 Atmosphere

Because our recent investigation of basic nitrite sodalite solid solution showed the possibility of high temperature intra cage reactions with carbon dioxide (6) we also study here the heterogeneous reaction behaviour of nitrite/nitrate sodalite in a CO_2 atmosphere.

After an isothermal heating of nitrite/nitrate sodalite at 973 K for a period of 30 min in a CO_2 stream of 5 liter/hr the initial nitrite/nitrate sodalite transforms into a carbonate enclathrated nitrate sodalite according to the following reaction step:

$$Na_8[AlSiO_4]_6(NO_2)(NO_3) + 0.5\,CO_2 \xrightarrow{973K} Na_8[AlSiO_4]_6(NO_3)(CO_3)_{0.5} + NO\uparrow + 0.25\,O_2\uparrow .$$

This reaction is mainly proceeding within the nitrite filled cages. Thus the reaction mechanism during this first heating step involves the total decomposition of the nitrite, which acts as the "reactive guest component" for the formation of sodium carbonate after the diffusion of CO_2 through the hexagonal cage "windows." During this reaction the enclathrated nitrate together with the new imbibed carbonate prevent the destruction of the sodalite

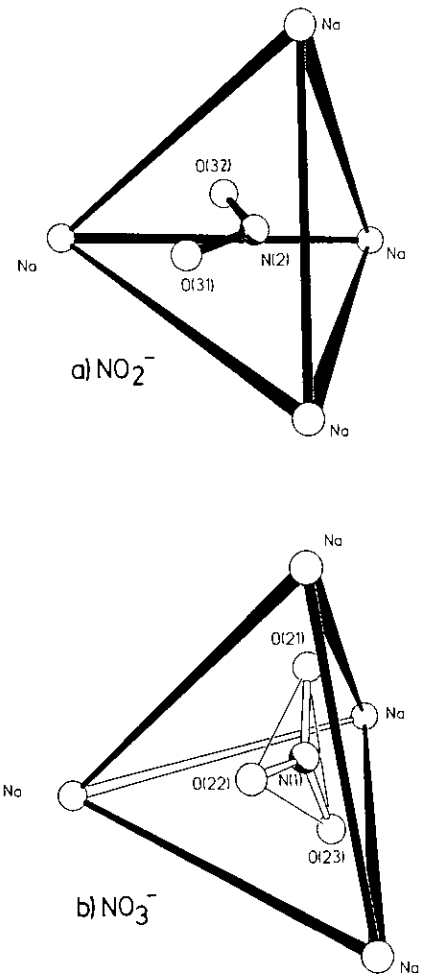

FIG. 4. The orientation of the nitrite (a) and the nitrate group (b) within the tetrahedral arrangement of the sodium cations inside the sodalite cages.

framework, i.e., both are acting as the "stabilizing guest components" of the mixed crystal.

A second heating procedure in CO_2 at 1073 K under the same conditions (30 min heating, CO_2 stream of 5 liter/hr) the high-temperature anion exchange reaction can be further extended, leading to the formation of a nonbasic carbonate sodalite according to the following reaction scheme:

$$Na_8[AlSiO_4]_6(NO_3)(CO_3)_{0.5} + 0.5\,CO_2 \xrightarrow{1073K} Na_8[AlSiO_4]_6(CO_3) + NO\uparrow + 0.75\,O_2\uparrow.$$

Now the nitrate is the "reactive guest," whereas all the imbibed carbonate keeps the framework stable.

Stepwise IR spectra of Figs. 5a and 5b, taken from the product after the first and the second reaction step clearly indicate the decomposition of a great amount of the nitrite during the first step already after 15′ tempering and the imbibition of carbonate due to the evaluation of the 1450 cm^{-1} absorption band for the asymmetric stretching mode of the CO_3^{2-} anion. At elevated temperatures during the second reaction step the decomposition of the nitrate occurs accompanied by further carbonate enclathration. The best results can be obtained when the samples were ground after 15′ of heating and than heated up for further 15′ at both temperatures.

The X-ray powder data of the resulting carbonate intercalated sodalites are given in Figs. 6a and 6b. An increase of the unit cell parameter can be stated during the observed reactions (a_0 = 8.994(1) Å for the first step and a_0 = 9.009(1) Å after the second step; the cell constant of the pure carbonate sodalite changes already after a few hours in air to a_0 = 8.996(1) Å according to the uptake of some water in the unfilled cages). Compared with the powder data of the nitrate/carbonate sodalite formed after the first heating process (Fig. 6a) the evaluation of an (100)-reflection as well as the (320)-reflection can be observed for the phase after the second reaction step. This indicates the total evaluation of a nosean-like alternating arrangement of the divalent carbonate-anions within 50% of the sodalite cages alongside 50% of unfilled cages.

The maximum amount of carbon dioxide, which can be incorporated in the initial nitrite/nitrate sodalite via high temperature anion exchange reactions is 50 mg CO_2 per gramme sodalite.

The observed thermal reaction behavior of nitrite/nitrate sodalite indicates, that sodalite solid solutions can be "constructed" with special chemical properties. These compounds are therefore acting as a model system for the use of sodalites as "reservoir minerals", an interesting new application route.

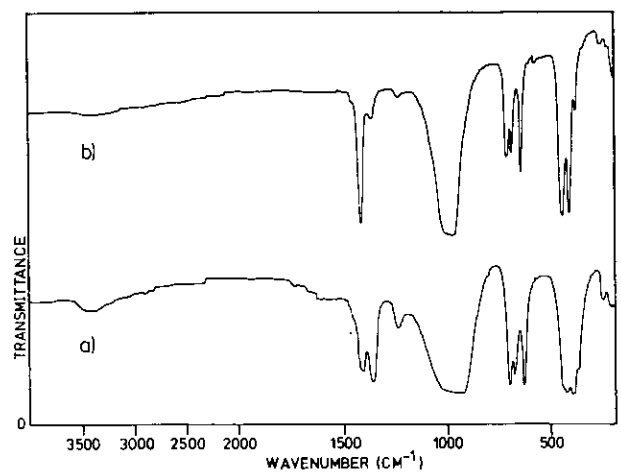

FIG. 5. IR spectroscopic characterization of the intracage reactions of nitrite/nitrate sodalite with CO_2: The carbonate imbibed reaction product after heating for 15′ at 973 K (a), and the same sample after a second heating procedure at 1073 K for 15′ (b).

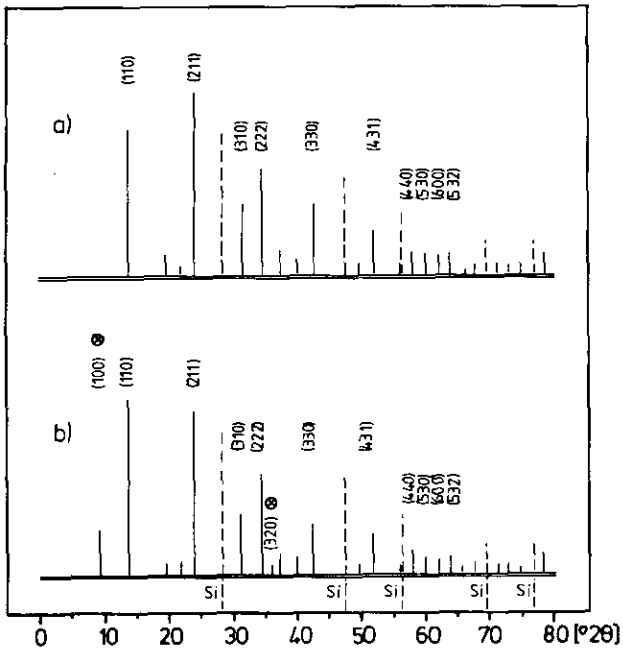

FIG. 6. X-ray powder diffraction diagrams of the carbonate imbibed reaction products: Nitrate/carbonate sodalite after heating of the initial nitrite/nitrate sodalite at 973 K for 30′ (a) and carbonate sodalite after an additional heating of sample (a) at 1073 K for 30′ (b). The new reflections are marked (⊗).

ACKNOWLEDGMENTS

The authors are gratefully indebted to Prof. Dr. W. Hoffmann (Münster) for valuable discussions. We are grateful to Dr. G. Engelhardt (Stuttgart) for carrying out the ^{23}Na MAS NMR measurement, to Dr. W. A. Buckermann (Münster) for the ^{29}Si MAS NMR spectrum and to Prof. Dr. J. Grobe for the permission to use the IR spectrometer in his laboratory.

REFERENCES

1. R. M. Barrer and J. F. Cole, *J. Chem. Soc. A* 1516 (1970).
2. F. Hund, *Z. Anorg. Allg. Chem.* **509,** 225 (1984).
3. J. Felsche and S. Luger, *Thermochim. Acta* **113,** 35 (1987).
4. J.-C. Buhl, G. Engelhardt, and J. Felsche, *Zeolites* **9,** 40 (1989).
5. J.-C. Buhl, *Thermochim. Acta* **189,** 75 (1991).
6. J.-C. Buhl, *J. Solid State Chem.* **94,** 19 (1991).
7. G. Geismar and U. Westphal, *Chem. Zeit.* **111,** 277 (1987).
8. A. Stein, G. A. Ozin, and G. D. Stucky, *J. Am. Chem. Soc.* **112,** 904 (1990).
9. A. Stein, G. A. Ozin, P. M. Macdonald, G. D. Stucky, and R. Jelinek, *J. Am. Chem. Soc.* **114,** 5171 (1990).
10. A. Stein, G. A. Ozin, and G. D. Stucky, *J. Am. Chem. Soc.* **114,** 8119 (1992).
11. M. T. Weller, G. Wong, C. L. Adamson, S. M. Donald, and J. J. B. Roe, *J. Chem. Soc. Dalton Trans.* **593** (1990).
12. J.-C. Buhl, Ch. Gurris, and W. Hoffman, *Ber. Dtsch. Miner. Ges.* **1,** 19 (1989).
13. J.-C. Buhl, *J. Solid State Chem.* **91,** 16 (1991).
14. A. F. Holleman and N. Wiberg, "Lehrbuch der Anorganischen Chemie." de Gruyter, Berlin/New York, 1985.
15. C. M. B. Henderson and D. Taylor, *Spectrochim. Acta Part A* **33,** 283 (1976).
16. G. Engelhardt, J. Felsche, and P. Sieger, *J. Am. Chem. Soc.* **114,** 1173 (1992).
17. M. Wiebke, G. Engelhardt, J. Felsche, P. Kempa, P. Sieger, J. Schefer, and P. Fischer, *J. Phys. Chem.* **96,** 392 (1992).
18. G. M. Sheldrick, "SHELX 76: Program for Crystal Structure Determination." Cambridge, 1976.
19. "International Tables for X-Ray Crystallography," Vol. 4. Kynoch Press, Birmingham, 1974.
20. J. Löns and H. Schulz, *Acta Crystallogr.* **23,** 434 (1967).
21. M. I. Kay and B. C. Frazer, Acta Crystallogr. **14,** 56 (1961).
22. S. Göttlicher and C. D. Knöchel, Z. Kristallogr. **148,** 101 (1978).
23. S. Göttlicher and C. D. Knöchel, *Acta Crystallogr. Sect. B* **36,** 1271 (1980).
24. P. Kempa, G. Engelhardt, J.-C. Buhl, J. Felsche, G. Harvey and C. Baerlocher, *Zeolites* **11,** 558 (1991).
25. P. Sieger, M. Wiebke, J. Felsche, and J.-C. Buhl, *Acta Crystallogr. Sect. C* **47,** 498 (1991).